J Incl Phenom Macrocycl Chem (2008) 60:103–113
DOI 10.1007/s10847-007-9358-4

ORIGINAL ARTICLE

Enantiodiscrimination of equol in β-cyclodextrin: an experimental and computational study

Elena Alvira · Jose A. Mayoral · Jose I. García

Received: 8 January 2007 / Accepted: 27 July 2007 / Published online: 14 September 2007

Abstract The interaction between the equol enantiomers and β-cyclodextrin is studied by molecular mechanics and molecular dynamics calculations. The chromatographic retention order is determined by these theoretical methods and compared with experimental findings. In the molecular mechanics calculations, the simultaneous relaxation of the host and the guest molecules is allowed, both in a vacuum and in aqueous solution. In the molecular dynamics calculations, the interaction energy between each enantiomer and the cavity is determined carrying out a simulation of 12 trajectories with different initial conditions at constant temperature (293 K), and minimising the energy of the structures extracted along the trajectories. To determine the preferential binding site and orientation of each guest molecule, the numerical density of presence in a volume element is calculated and compared with regions of maximum enantioselectivity. The more stable complex predicted in both cases is formed with *R*-equol, in agreement with experimental results.

Keywords Chemical physics · Experimental research · Computer simulation · Molecular mechanics · Molecular dynamics

E. Alvira (✉)
Departamento de Física Fundamental II, Universidad de La Laguna, 38206 La Laguna, Tenerife, Spain
e-mail: malvira@ull.es

J. A. Mayoral · J. I. García
Instituto de Ciencia de Materiales de Aragón, Facultad de Ciencias, Universidad de Zaragoza, 50009 Zaragoza, Spain

Introduction

In order to explain the properties of a system, models can be used to allow approximate theories to be constructed. Microscopic models try to reproduce the processes at the atomic level based on data such as macroscopic properties and experimental findings. Among microscopic methods, computer simulation is one of the most extensively applied because developments in computer technology enable its application to progressively more complicated systems. There are no rules about which simulation method (e.g. molecular dynamics, Monte Carlo method) is best applied to a process, but some factors influencing the choice are: the details of the molecular system (size and structure), data available, physico-chemical properties or even the information to be determined [1–4].

Cyclodextrins (CyDs) are macrocyclic molecules composed of glucose units (7 for β-CyD) forming truncated cone-shaped compounds and their ability for catalysis and chiral recognition is mainly due to the formation of inclusion complexes [5, 6]. The type of molecules that can be introduced in the cavity to form an inclusion complex, depends mainly on geometric factors rather than on chemical properties, however these are evidently not the only factors. Normally each guest is considered as an individual case when binding to the host and the interaction for each substrate is studied as a unique case [7, 8].

In recent years we have studied the interaction between β-CyD and some guest molecules [9–13], equol is one of the molecules considered, it possesses an asymmetric carbon atom, i.e. it is a chiral compound. Equol is an 'oestrogen-like' isoflavonoid compound and its nuclear magnetic resonance spectrum is identical to that of 3,4-dihydro-3-(4-hydroxy-phenyl)-2*H*-1-benzopyran-7-ol

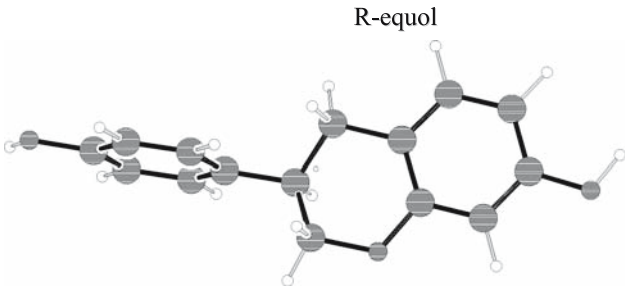

Fig. 1 Structure of *R*-equol molecule

(Fig. 1). It is a potent inhibitor of the Na–K–Cl cotransport system and employed in pharmacological applications [14]. Using a molecular modelling method (based on molecular mechanics) we studied the interaction between each equol enantiomer and β-CyD by determining the potential surfaces, energy and structures of inclusion complexes [12]. We applied the results to predict the elution order corresponding to the chiral discrimination of equol by β-CyD. In that work we did not take into account the relaxation of the molecules and the environment in which the process occurs. The influence of solvation effects and structural relaxation of the host and the guest molecules are determined by molecular mechanics (MM) calculations in the present work. However, MM does not facilitate other data like the molecular trajectory, preferential binding sites on the host or the preferred orientation of the guest inside the cavity [15, 16].

Molecular dynamics (MD) is based on the resolution of classical equations of motion of a set of molecules in order to determine the trajectory of the particles depending on the initial conditions of the system. By treating the results generated in this process with statistical methods one can obtain more detailed information about the formation of the complexes [4]. To consider the effect of conformational adaptation of the guest to the cavity, the structure can be relaxed during the trajectory, for this MM calculations are carried out. In one case the interaction energy between each enantiomer and the cavity is determined by structural relaxation, whereas in another method the interaction energy is considered to be the mean obtained for different rigid configurations of each equol enantiomer [8]. Once the trajectories for each configuration are determined, the mean total energy represents the average intermolecular energy for different atomic positions of the guest molecule. The aim of the present study is to compare the results obtained for the enantioselectivity of equol in β-CyD, by these two methods (MM, MD), and also with the experimental findings. In "Experimental section" we present the experimental results, in section "Simulation methods" the theoretical methods and their main results in section "Results and discussion".

Experimental section

HPLC experiments were carried out in the following conditions. About 0.5 mg (2.064 mmol) of equol (either racemic or enantiomerically pure) were dissolved in 50 µL of pure ethanol. A 5 µL sample of this solution was analysed by HPLC.

HPLC analysis (Waters): Kromasil C18 (5 µm, 150 × 40 mm, 100 Å) at 313 K; ammonium acetate buffer (0.05 M, pH = 4.7)/methanol (85:15) as eluent (0.8 mL/min); UV detection: 280 nm. In the case of chiral recognition experiments, β-cyclodextrin (0.05 M) was added to the mobile phase.

Retention times: 45.1 min. (racemic equol); 22.6 min (*R*-enantiomer in the presence of β-CyD); 23.9 min (*S*-enantiomer in the presence of β-CyD).

Estimating the elution order when the chiral discriminator is in the mobile phase is not a straightforward task. The capacity ratio, *k*', to which the retention time is directly related, depends on several equilibria that involve the stationary phase and the chiral selector in the mobile phase:

$$\text{Equol} + \beta\text{-CyD} \overset{K_C}{\rightleftarrows} [\text{Equol}-\beta\text{-CyD}]$$

Mobile phase inclusion equilibrium

$$\text{Equol}_m \overset{K_E}{\rightleftarrows} \text{Equol}_s$$

$$[\text{Equol}-\beta\text{-CyD}]_m \overset{K_I}{\rightleftarrows} [\text{Equol}-\beta\text{-CyD}]_s$$

Mobile phase/stationary phase equilibria

From experimental data we know that the elution time is much longer in the absence of β-CyD, so we can conclude that $K_E > K_I$. Furthermore, no free equol is detected in the presence of β-CyD in the experimental conditions, so $K_C[\beta\text{-CyD}] >> K_E$. We can then to establish that $K_C[\beta\text{-CyD}] >> K_E > K_I$. Concerning the behaviour of both enantiomers, it is evident that K_E must be the same for both, so this constant does not influence the relative retention times. Given the relative importance of the different equilibria, it seems reasonable to conclude that the main term influencing the chromatographic separation will be the difference between the inclusion complex constants, K_C, for the *R*- and *S*-enantiomers of equol. If this hypothesis is true, the most complexed enantiomer will appear a shorter retention times.

Simulation methods

Molecular mechanics calculations

Calculation of different equol–β-CyD complexes was also carried out by complete relaxation from different initial

configurations, using two different molecular mechanics force fields, namely MM2 [17, 18] and Amber, [19, 20] as implemented in the MacroModel package [21]. The initial structures were chosen to be those leading to minimum energies in the rigid-body molecular mechanics simulations [12], which corresponded to one *R*- and two *S*-enantiomer-inclusion complexes. Furthermore, solvent effects were also taken into account through the Generalized Born/Surface Area (GB/SA) continuum solvation model [22, 23], as implemented in MacroModel.

Molecular dynamics calculations

The atomic coordinates of β-CyD were taken from the literature [24] and the geometry of equol was calculated using the AM1 semi-empirical Hamiltonian included in the MOPAC 6.0 package [25]. Minimum energy conformations for equol are assumed to calculate the interaction between the guest molecule and CyD. Although there is no one single geometry that minimises the energy of equol in vacuo, there are other conformations with small differences in the atomic positions that have a similar energy. In the present study of enantiodiscrimination based on MD, we considered three different geometries for each equol enantiomer: *R*1, *R*2 and *R*3 (or *S*1, *S*2 and *S*3). Every molecule of equol has the same mass, but the differences in the atomic positions between the configurations give rise to different principal moments of inertia.

We place the origin of the reference system at the centre of mass of the cavity and the space-fixed frame over the principal axis (in which the inertia tensor is diagonal) of the CyD. The position of equol is given by the coordinates of its centre of mass and the orientation of this molecule is defined by the relation between its principal body-fixed system and the axis system fixed in space.

To integrate the equations of motion it is necessary to establish the initial conditions of the guest molecule: position, orientation (Euler angles) and velocities. The magnitude of the initial velocities depends on the temperature of the process but the directions of the translational and rotational velocities in each trajectory, as well as the initial centre of mass position are determined randomly. In the present study we do not necessarily consider its minimum energy orientation in every position of its centre of mass. Basically, there are four relative positions between the molecules: the centre of mass of the guest near each face of the CyD and with one of the extremes of equol (simple or double rings) inside the cavity. The initial structures considered for each process are represented in Fig. 2. Each possibility is represented by a number (1, 2, 3 and 4) and the different initial conditions with a letter (a, b and c). All the molecules of equol have the same centre of mass position and molecular orientation but differ in their atomic positions.

We have calculated 12 trajectories. The simulation time for each one is 2 ns with a step of 1 fs and the configuration and energies (kinetic and potential) were written every 100 steps. The software we used is an in-house program written in Fortran and, to perform constant temperature molecular dynamics (293 K), the equations of motion were integrated numerically using a variant of the leap-frog scheme (proposed by Brown and Clarke) [26], constraining the rotational and translational kinetic energies separately [27].

In rigid-body dynamics the molecular motion can be decomposed into two completely independent parts, translational motion of the centre of mass and rotation about the centre of mass. A basic result of classical mechanics is that the former is governed by the total force acting on the body, whereas the latter depends on the total applied torque. The total force acting on the body is determined as the sum of the interactions between the atoms of both molecules. The interaction energy and therefore the force between the molecules are represented by the contributions of the electrostatic and van der Waals terms, because inside the cavity there are no hydrogen bonds [12]. A 6–12 function is used to simulate the van der Waals interaction, and the force between charges and thus the corresponding electrostatic potential are calculated by the Coulomb formula [12, 13].

To consider the effect of conformational adaptation of the guest to the cavity, the MM calculations were carried out with the MM2 force field. The energy minimising structures were extracted along the trajectories. However in consequence of the probability density of presence, the interaction energies corresponding to the configurations in which the complex remains for longer period in the simulation, contribute mainly to the mean energy of the simulation.

Two methods were applied to determine the average energy for *R*- and *S*-equol, and then the elution order:

(a) Starting from the *R*1 and *S*1 configurations, the effect of conformational adaptation of the guest to the cavity was considered by carrying out MM calculations with the most probable structures.
(b) The interaction energy for every configuration of each enantiomer was averaged, i.e. for 36 trajectories.

To determine the preferential binding site and orientation of the guest molecule the number densities of presence in a volume element were calculated. We defined a grid in which the distance between two consecutive points is 0.5 Å and the number of guest positions in each volume element is the resulting number density for each trajectory and for the guest [15, 16]. The position probability density is calculated dividing the number density in a volume element by the total guest's centre of mass positions. The most

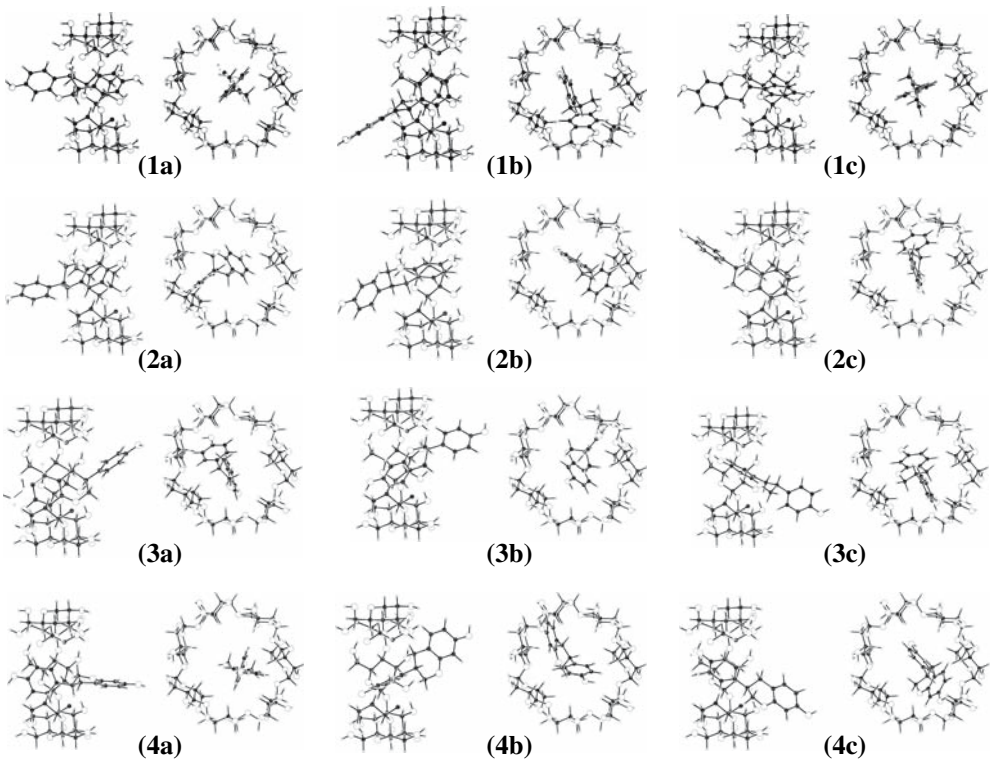

Fig. 2 Starting configurations for the simulations

probable orientation is that of the position with greater number density.

The position probabilities for *R*- and *S*-equol were compared with the potential surface corresponding to the regions of maximum discrimination. The potential energy surface was calculated for each enantiomer and the maximum chiral discrimination localised in the regions with greatest differences in energy. To determine this surface, a grid with sides of 0.5 Å was defined. The guest centre of mass was then placed at each grid point and the molecule rotated by means of Euler angles. The potential energy at each position was usually considered as the lowest energy at each grid point [13], but in this case the enantiomers of equol did not in general adopt the lowest energy configuration in each position of the trajectory. Therefore to compare with the results of molecular dynamics calculations, the average Boltzmann energy corresponding to different guest orientations (726) was assigned to each grid point [16].

Results and discussion

Molecular mechanics calculations

In order to test if the complete relaxation of the host-guest complex may change the complexation preferences, and hence the chiral discrimination, the most stable equol–*β*-CyD complexes found in the MM simulations [12] were used as starting points to a complete MM energy minimisation. In the case of the *S*-enantiomer, two different starting complexes (*S*-I and *S*-II) were considered, because its close energy. The resulting structures are shown in Fig. 3, and the corresponding complexation energies are gathered in Table 1.

Solvent effects may, in principle, change both the geometries and the relative energies of the equol–*β*-CyD complexes. Therefore, we also considered the minimisation process in the presence of a solvent, namely water, through the GB/SA solvation method. The corresponding minimised structures are shown in Fig. 3, where it is difficult to compare the in vacuo and solution geometries by visual inspection. The rms deviation in the atomic positions of in vacuo and solution structures in the Amber* and the MM2* force fields is about 0.14 Å and 0.48 Å respectively.

The results of calculated energies (Table 1) show that in all cases, the *R*-enantiomer (entry 1) is more strongly binded to the CyD than the *S*-enantiomer (entries 2 and 3), in agreement with the experimental results. The comparison between the Amber* and the MM2* force fields indicates that the latter exhibit a greater preference for the *R*-enantiomer complexation in vacuo. However, in aqueous solution the difference between both force fields is smaller. In general, solvent effects tend to approximate the relative energies of the equol–*β*-CyD complexes confirming the

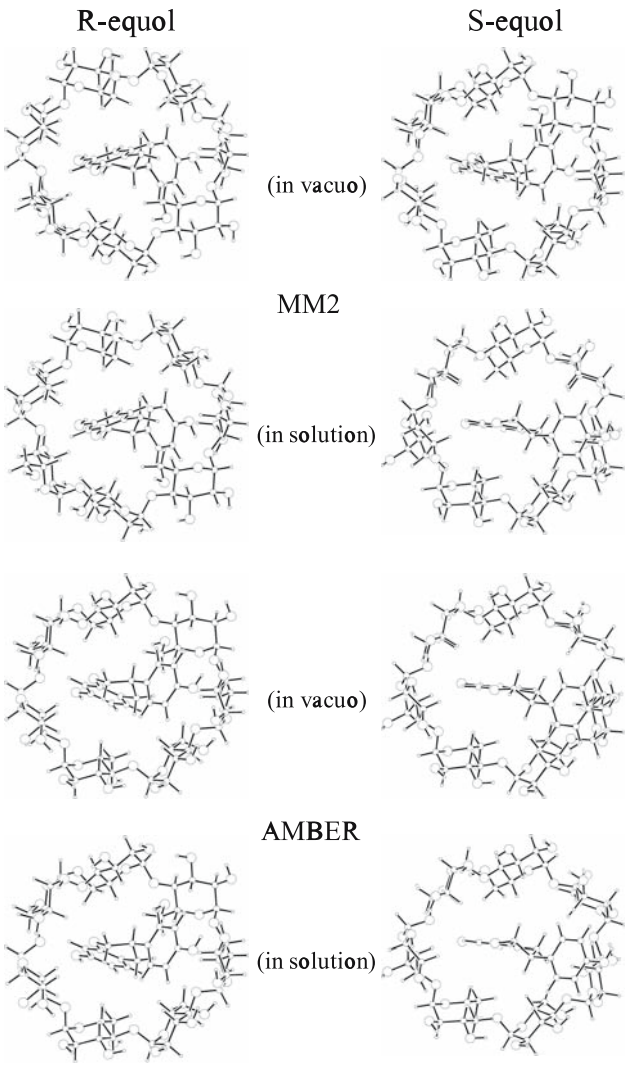

Fig. 3 Minimum energy geometries of the *R*- and *S*-equol-CyD inclusion complexes, optimised in vacuo and in aqueous solution (GB/SA) with the MM2 and Amber force fields

Table 1 Calculated relative energies (in kcal mol^{-1}) of the equol–*β*-CyD complexes, optimised using two different force fields, in vacuo and in aqueous solution

Entry	Config.	Solvation	ΔE_{MM2}	ΔE_{amber}
1	*R*	N	0.0	0.0
		Y	0.0	0.0
2	*S*-I	N	7.0	9.7
		Y	3.7	3.1
3	*S*-II	N	17.7	29.3
		Y	12.6	15.6

results founded in [12]: in vacuo the different contribution of the van der Waals term to the total energy for each enantiomer is increased by the Coulombic forces which also cause the difference between the most stable position of *R*- and *S*-equol. Solvation makes the contribution of the

Table 2 The mean potential energy V_T, van der Waals contribution V_{LJ} and Coulombic term V_{elec} (in kcal/mol) for the simulation of *R*1, *R*2 and *R*3 equol

Process	*R*1			*R*2			*R*3		
	V_T	V_{LJ}	V_{elec}	V_T	V_{LJ}	V_{elec}	V_T	V_{LJ}	V_{elec}
1a	−20.90 ± 1.83	−15.12 ± 1.27	−5.78 ± 1.03	−19.54 ± 1.57	−15.16 ± 1.06	−4.38 ± 0.98	−19.71 ± 1.12	−15.44 ± 0.81	−4.27 ± 0.86
1b	−20.03 ± 2.24	−14.66 ± 1.45	−5.37 ± 1.29	−19.60 ± 2.00	−14.98 ± 1.15	−4.62 ± 1.21	−19.23 ± 2.07	−15.24 ± 1.16	−3.99 ± 1.31
1c	−20.14 ± 2.34	−14.54 ± 1.77	−5.60 ± 1.15	−19.83 ± 1.21	−15.35 ± 0.84	−4.48 ± 0.99	−19.50 ± 1.46	−15.26 ± 0.91	−4.24 ± 1.06
2a	−17.97 ± 1.53	−11.64 ± 1.44	−6.33 ± 1.51	−16.26 ± 1.64	−11.00 ± 1.78	−5.26 ± 2.58	−16.65 ± 1.31	−10.70 ± 1.64	−5.95 ± 1.47
2b	−18.17 ± 1.37	−11.37 ± 1.31	−6.80 ± 1.08	−16.67 ± 1.59	−10.52 ± 1.52	−6.15 ± 1.79	−16.25 ± 1.77	−11.07 ± 1.62	−5.18 ± 1.53
2c	−18.15 ± 1.62	−11.68 ± 1.42	−6.47 ± 1.39	−16.44 ± 1.70	−10.78 ± 1.66	−5.66 ± 2.32	−16.37 ± 1.65	−10.64 ± 1.67	−5.73 ± 1.72
3a	−21.21 ± 1.34	−15.29 ± 1.11	−5.92 ± 0.72	−19.91 ± 1.43	−15.16 ± 0.84	−4.75 ± 1.05	−19.78 ± 0.91	−15.49 ± 0.71	−4.29 ± 0.81
3b	−20.08 ± 1.97	−14.52 ± 1.87	−5.56 ± 0.94	−19.35 ± 1.74	−13.20 ± 1.23	−6.15 ± 1.35	−19.79 ± 1.91	−13.73 ± 0.95	−6.06 ± 1.32
3c	−21.07 ± 1.45	−15.24 ± 1.19	−5.83 ± 0.81	−19.80 ± 1.49	−14.95 ± 0.91	−4.85 ± 1.00	−19.80 ± 1.04	−15.37 ± 0.73	−4.43 ± 0.85
4a	−18.02 ± 1.69	−11.55 ± 1.62	−6.47 ± 1.39	−16.23 ± 2.20	−10.62 ± 1.77	−5.61 ± 2.27	−16.35 ± 1.54	−10.96 ± 1.63	−5.39 ± 1.78
4b	−18.17 ± 1.42	−11.59 ± 1.40	−6.58 ± 1.37	−16.61 ± 1.68	−10.48 ± 1.51	−6.13 ± 1.83	−16.16 ± 1.58	−11.09 ± 1.63	−5.07 ± 2.11
4c	−18.15 ± 1.48	−11.69 ± 1.23	−6.46 ± 1.40	−16.49 ± 1.54	−11.09 ± 1.68	−5.40 ± 2.01	−16.29 ± 1.79	−10.91 ± 1.84	−5.38 ± 2.06

electrostatic term decrease with respect to the vacuo, in this case the van der Waals term is the main contributor to the interaction energy and also determines more similar stable positions for each enantiomer. In all cases the *R*-enantiomer complex is largely favoured, which is again in agreement with that expected from our chiral discrimination model.

The chromatographic retention order predicted by this theoretical method agrees with the experimental findings, but MM calculations cannot justify why equol tends to remain inside the cavity and then no free equol is detected in the presence of β-CyD in the experimental conditions. The preferential binding site and orientation of equol when the guest molecule approaches the β-CyD is facilitated by MD calculations.

Molecular dynamics calculations

Simulation for R-equol

The evolution of the system in each trajectory and its resultant average energy, are different because the initial conditions determine the integration of the equations of motion. These initial conditions affect the simulation in a different way, while the velocities hardly influence the number densities and the average energy of the process, the greatest differences in these values are due to the initial configuration.

In order to elucidate what happens with the different initial conditions, the mean energy of each process, as well as the mean electrostatic and van der Waals contributions, with their overall average values over the simulation are given in Table 2. Starting from the configurations 1a, 1b, 1c, 3a, 3b and 3c the energy variations are bigger and the mean energy lower than that of the configurations 2a, 2b, 2c, 4a, 4b and 4c, the difference between them being about 2.5 kcal/mol. Moreover the average electrostatic term is nearly the same for each process and the difference in the potential energy is due mainly to the Lennard-Jones contribution.

In the simulations 1a, 1b and 1c the position of the centre of mass (near one face of the cavity) and the initial velocities are different, and the difference between the mean energies is about 0.5 kcal/mol. In the simulations 3a, 3b and 3c the centre of mass of the guest is near the opposite face of the cavity, in addition to the random initial

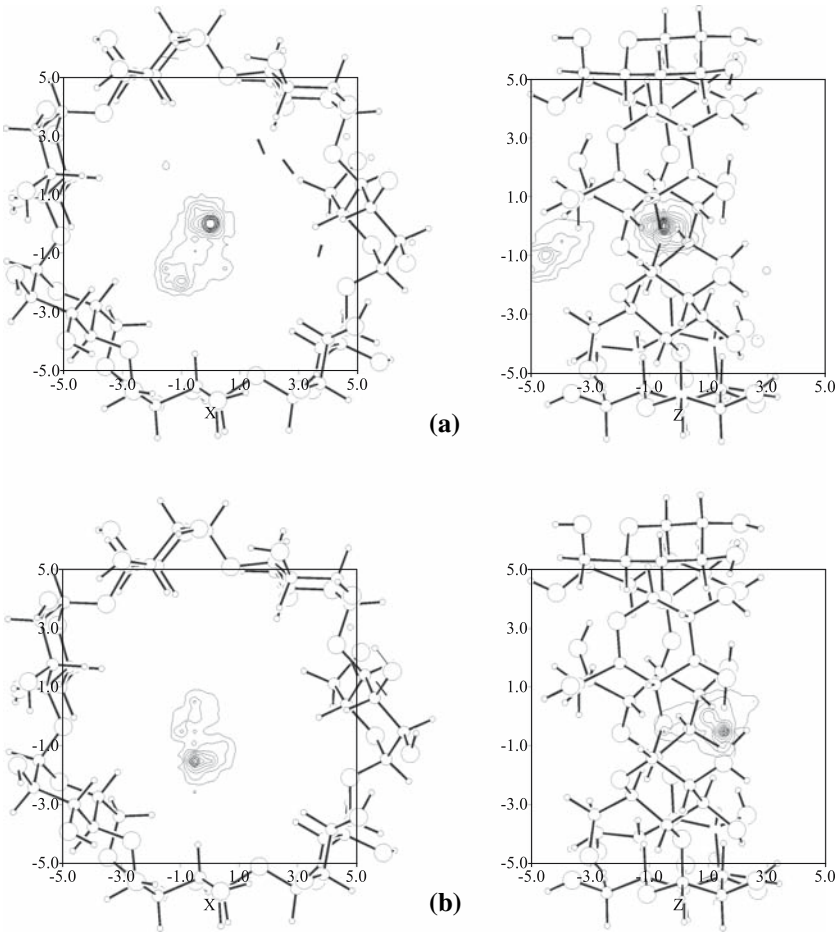

Fig. 4 (**a**) Probability density at each position in the simulation of *R*-equol. (**b**) Same as (**a**) for *S*-equol

velocities and the difference between these mean energies and those of simulations 1 being about 0.5 kcal/mol. In both cases the relative orientation of the guest with respect to the CyD is similar: the double ring is 'to the left' in Fig. 2. For simulations 2 and 4 the differences are even smaller (about 0.2 kcal/mol.) and in these cases the double ring of the equol is pointing towards the right in Fig. 2. If the mean energies of processes 1 and 3 differ in about 2.5 kcal/mol from those of processes 2 and 4, it seems that it depends mainly on the initial orientation. Therefore the mean energies of the processes depend above all on the initial orientation, more than the starting velocities and position of the guest's centre of mass. Every configuration of *R*-equol showed this characteristic: the mean potential energy in each trajectory tends towards two values, depending on the initial orientation of the guest with respect to the CyD (Table 2).

In order to determine the preferential binding site of *R*-equol in the simulation, the densities of presence in a volume must be calculated. The results for *R*1, *R*2 and *R*3 are very similar: the most probable position for the guest is the centre of the cavity (12.10%) although there is another possible position, outside the cavity axis near the narrow rim (3.80%) (Fig. 4a). However, there are other complex structures near to the preferential binding site, with small variations in guest position and orientation that have a similar interaction energy and therefore also contribute considerably to the mean energy. The total probability of presence is about 40% around the cavity centre, and about 25% near the narrow rim. The remaining probabilities of presence out of these positions are smaller than 1%.

The preferred orientation in trajectories 1 and 3 is represented in Fig. 5a and for the others, in Fig. 5b, in both cases the equol tends to introduce its double ring inside the CyD. We have already calculated the penetration potential as the variation of the potential energy along the cavity axis, noting that it presented two relative minima depending on the position of the guest's centre of mass: near the centre of the cavity or near the narrow rim of the CyD. In each case the orientation of the guest was different (Fig. 3b and d) [12] The dynamics simulation of the system shows this characteristic because the complex tends towards one of these two configurations and consequently, the two possible mean energies of the processes are at approximately the values corresponding to these minima. Therefore, in the simulation the *R*-equol locates its centre of mass near the cavity centre for the longest period (inclusion complex), but the configuration of this complex during the main part of the simulation time does not correspond to that of the minimum energy.

To minimise the mean energy of the simulation we let relax the complexes using a MM2 force field (Fig. 5). It

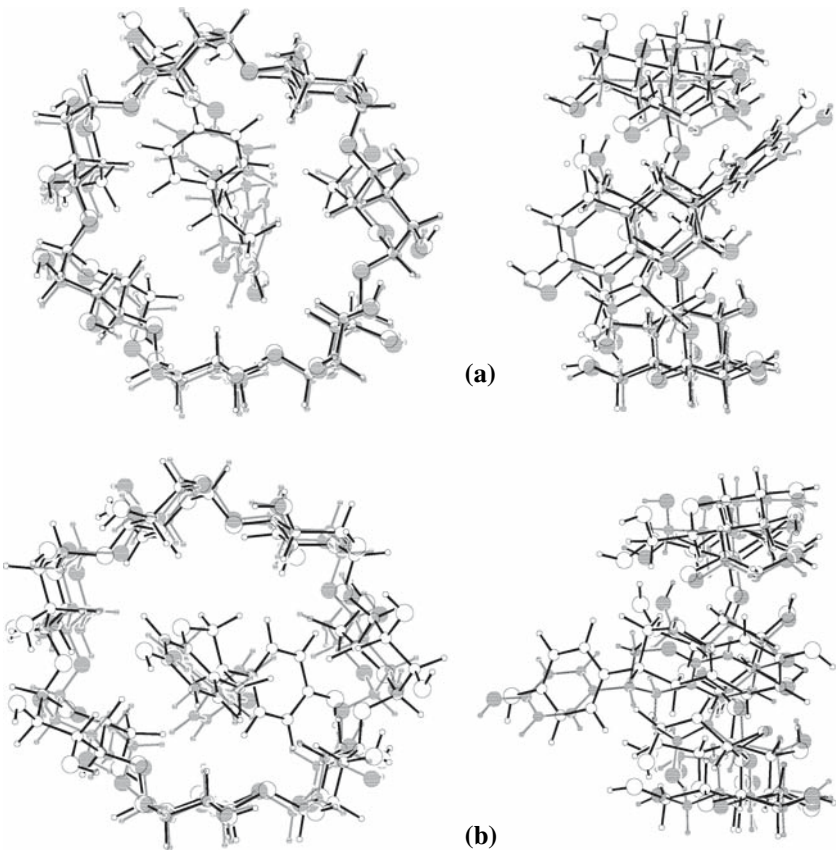

Fig. 5 (**a**) Configuration of the complex formed by β-CyD and *R*-equol in trajectories 1 and 3 after minimising the energy. It has been included in grey the started structure of the complex. (**b**) Same as (**a**) for the complex formed in trajectories 2 and 4

can be seen that, while the CyD hardly modifies his atomic positions, the greatest differences correspond to the equol. The rms deviation in the atomic positions (heavy atoms only) is about 0.24 Å and 0.57 Å respectively. The mean total energy of the system calculated by MD is smaller than that obtained in [12], because in MD only the configurations adopted by the guest along the trajectory contribute to the average.

Simulation for S-equol

For *S*-equol, the mean total energy in each process also tends towards two values depending on the initial orientation of the guest (Table 3). To understand the behaviour of the mean values of total energy, van der Waals and electrostatic contributions for the simulation of *S*-equol, we studied the probability of presence of this enantiomer inside the cavity. Fig. 4b indicates that the most probable position is the guest lying outside the cavity axis, between the middle of the cavity and the broader rim (13.90%), although there is another feasible position near the centre of the cavity (3.35%). However, other similar complex structures that contribute to the total probability of presence in these regions should be taken into account, with small variations in the guest orientation or centre of mass position and consequently the intermolecular energy. The approximate results obtained are 25% near the cavity centre and 40% between the middle of CyD and the broader rim; in other positions the probability is less than 1%.

The differences in the mean energy are due mainly to the coulombic term, because in the region where the guest remains for the longest period in the simulation, this term presents a variation of about 4 kcal/mol at positions of the guest centre of mass separated by less than 1 Å [12].

In the inclusion complex of minimum energy formed by *β*-CyD and *S*-equol, the guest centre of mass is located near the narrower rim of the cavity, along with the single ring of the equol [12, 13]. In MD simulation the preferential orientation of *S*1 for trajectories 1 and 3 corresponds to the single ring of equol pointing towards the broader rim of the CyD (Fig. 6a), Fig. 6b represents the preferential guest orientation in trajectories 2 and 4. The final optimised structures are also represented in Fig. 6, the rms deviation in the atomic positions (heavy atoms only) being about 0.23 and 0.29 Å.

Chiral discrimination

The elution order may be determined by two different ways depending on the method used in MD to calculate the

Table 3 The mean potential energy V_T, van der Waals contribution V_{LJ} and Coulombic term V_{elec} (in kcal/mol) for the simulation of *S*1, *S*2 and *S*3 equol

Process	S1			S2			S3		
	V_T	V_{LJ}	V_{elec}	V_T	V_{LJ}	V_{elec}	V_T	V_{LJ}	V_{elec}
1a	−21.16 ± 1.09	−14.78 ± 1.01	−6.38 ± 0.53	−18.16 ± 0.99	−16.23 ± 0.97	−1.93 ± 0.94	−17.84 ± 0.64	−16.48 ± 0.66	−1.36 ± 0.76
1b	−21.15 ± 2.3	−14.83 ± 1.37	−6.32 ± 1.31	−18.29 ± 0.77	−16.36 ± 0.75	−1.93 ± 0.86	−16.61 ± 1.04	−15.67 ± 0.76	−0.94 ± 1.04
1c	−21.20 ± 1.00	−14.81 ± 0.93	−6.39 ± 0.51	−17.91 ± 1.56	−15.97 ± 1.43	−1.94 ± 0.97	−16.71 ± 0.66	−13.91 ± 0.59	−2.80 ± 0.35
2a	−17.49 ± 0.91	−15.04 ± 1.21	−2.45 ± 1.03	−15.22 ± 0.91	−13.23 ± 1.11	−1.99 ± 1.00	−15.85 ± 1.47	−13.48 ± 1.49	−2.37 ± 2.20
2b	−17.11 ± 1.00	−14.98 ± 0.96	−2.13 ± 0.78	−15.44 ± 1.01	−12.07 ± 1.56	−3.37 ± 1.13	−15.77 ± 1.39	−13.29 ± 1.80	−2.48 ± 1.20
2c	−16.51 ± 1.52	−14.25 ± 1.60	−2.26 ± 1.46	−15.21 ± 1.06	−11.39 ± 1.05	−3.82 ± 0.88	−15.94 ± 1.46	−13.16 ± 1.79	−2.78 ± 2.20
3a	−21.18 ± 1.31	−14.76 ± 1.17	−6.42 ± 0.50	−18.24 ± 0.89	−16.31 ± 0.87	−1.93 ± 0.86	−17.85 ± 0.62	−16.50 ± 0.64	−1.35 ± 0.75
3b	−21.14 ± 1.05	−14.77 ± 1.01	−6.37 ± 0.44	−18.17 ± 0.98	−16.21 ± 1.04	−1.96 ± 0.87	−17.81 ± 0.78	−16.47 ± 0.74	−1.34 ± 0.77
3c	−21.10 ± 1.12	−14.73 ± 1.05	−6.37 ± 0.44	−18.28 ± 0.73	−16.35 ± 0.76	−1.93 ± 0.83	−17.82 ± 0.71	−16.46 ± 0.77	−1.36 ± 0.77
4a	−16.99 ± 1.18	−14.63 ± 1.48	−2.36 ± 1.33	−15.24 ± 1.47	−12.30 ± 1.28	−2.94 ± 1.43	−15.26 ± 1.93	−12.82 ± 1.77	−2.44 ± 2.30
4b	−16.86 ± 1.40	−14.90 ± 0.99	−1.96 ± 0.79	−15.74 ± 1.14	−10.40 ± 1.07	−5.34 ± 1.06	−15.39 ± 1.04	−14.14 ± 0.97	−1.25 ± 1.16
4c	−16.35 ± 1.83	−14.42 ± 1.51	−1.93 ± 1.58	−15.24 ± 1.33	−12.20 ± 1.12	−3.04 ± 1.51	−15.57 ± 1.47	−13.81 ± 1.48	−1.76 ± 1.92

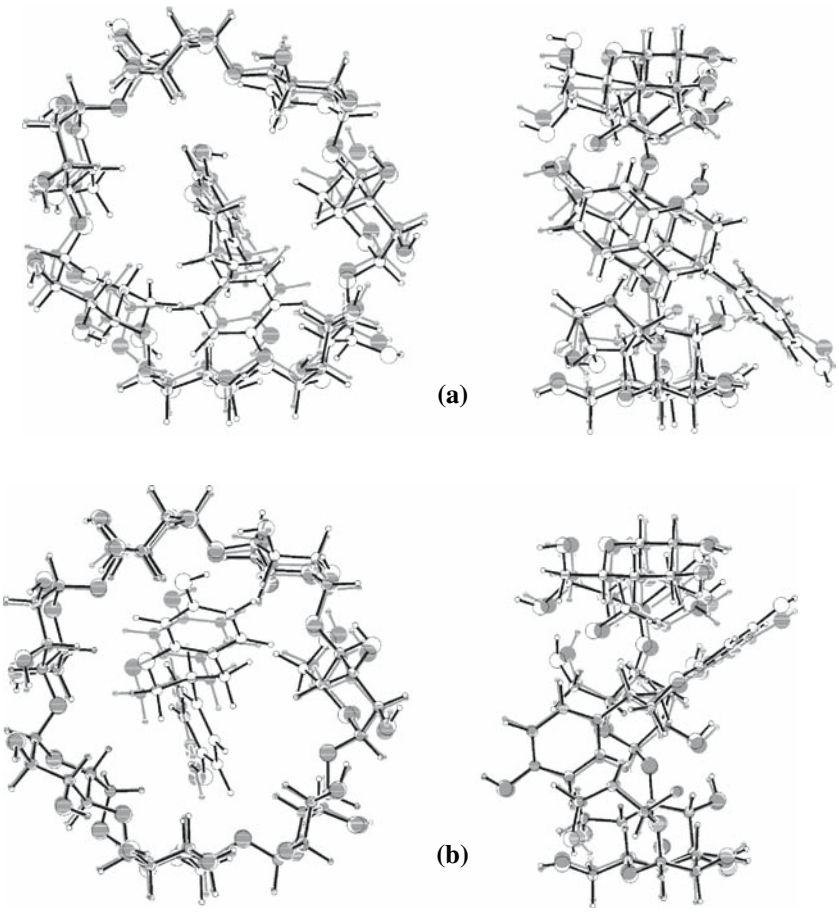

Fig. 6 (**a**) Configuration of the complex formed by β-CyD and *S*-equol in trajectories 1 and 3 after minimising the energy. The initial structure of the complex has been included in grey. (**b**) Configuration for the complex formed in trajectories 2 and 4

average energy for each enantiomer: with the relaxed structures or with different rigid conformations.

(a) To determine the mean energy with the relaxed structures, the weighted average for the most probable configurations was calculated and the results obtained are −19.65 kcal/mol for *R*1 and −19.34 kcal/mol for *S*1. Therefore the more stable complex is formed with the *R*-enantiomer and the difference between the energies is about 0.31 kcal/mol.

(b) If we calculate the average value of 36 trajectories for each enantiomer we obtain −18.46 kcal/mol for *R*-equol and −17.44 kcal/mol for *S*-equol. Therefore, we can conclude that in this case the *R*-enantiomer is also more stable and the difference between the energies is about 1.02 kcal/mol. If we consider each configuration separately, we obtain the same retention order because the mean total energy for *R*1, *R*2 and *R*3 is lower than for *S*1, *S*2 and *S*3. However, the difference between these energies varies from 0.32 kcal/mol (*R*1 and *S*1) to 1.46 kcal/mol (*R*3 and *S*3).

These results are thus in agreement with the experimental elution order and our hypothesis on the importance of the inclusion complex constants on the relative retention times. The influence of molecular relaxation on the retention order is widely confirmed in molecular mechanics calculations, where small differences in the interaction energy can determine the most stable enantiomer. However, there are many theoretical studies carried out by rigid-body molecular dynamics, that can produce results in accord with experiment depending on the simulation time [8]. In the present work the results obtained from both methods are similar because the equol moves in the trajectory about 0.1 ns until it reaches a stable configuration in which it remains for the longest time in the simulation, being therefore the time a decisive factor to produce accurate results.

It is clear that equol preferentially becomes located inside the cavity, but with each enantiomer at different positions. To know if the position probability of each molecule corresponds to zones of maximum enantioselectivity, the potential surfaces for *R*- and *S*-equol, as well as their difference, have been determined. To represent the difference between the average energies of *R*- and *S*-equol at each point of the XY plane along the cavity axis, the range of variation of the Z axis can be divided into four parts, each of about 2.5 Å. For each region we

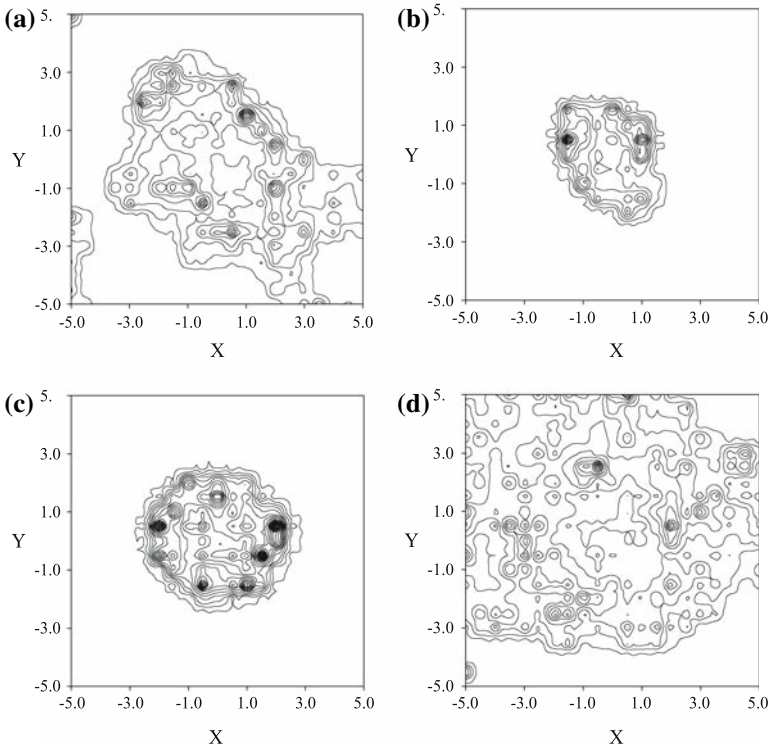

Fig. 7 Difference between the energies of *R*- and *S*-equol at each point on the XY plane (**a**) near the narrow rim of the CyD, (**b**) and (**c**) inside the cavity, (**d**) near the broader rim

determined the maximum energy difference in the interval of Z at every corresponding point on the XY plane. Fig. 7a represents positions of the guest centre of mass inside and outside the cavity, near the narrow rim of the CyD. Fig. 7b and c correspond to positions inside the CyD, and Fig. 7d is similar to 7a but near the broader rim of the CyD. The maximum chiral discrimination corresponds to positions of the guest centre of mass inside and near the cavity wall, not at the centre of the cavity, clearly different from the preferential location of the enantiomers. However this result is not true for other host-guest systems, in some cases the most enantiodifferentiating region of the macrocycle (the interior) is also where the analytes prefer to bind, as for the enantiomers studied by Lipkowitz et al. in [16]. That will depend individually on the host and the guest involved as well as on environmental effects. It is necessary the spatial agreement between the substrate binding site and regions of greatest enantiodifferentiation to ensure efficient chiral recognition in host-guest chemistry.

The finding that R-equol tends to locate near the centre of the cyclodextrin cavity whereas the less favoured S enantiomer locates off the cyclodextrin axis and nearer a rim (and also nearer more enantiodiscriminating regions of the cavity), suggests that much of the chiral discrimination in this system arises from more repulsive interactions for the less favoured enantiomer.

Conclusions

In this work we have studied the enantioselectivity of equol in β-CyD. The interaction energy between each enantiomer and the cavity was calculated by MM and MD. The more stable complex in both cases was formed with *R*-equol, in agreement with the experimental elution order observed, although the difference between the average total energies varies from one method to another.

In MD, the retention order is determined by two theoretical methods: either starting from different initial configurations for one enantiomer and averaging the trajectories and energies obtained, or relaxing by MM the structures most likely to minimise the energy. The probability of presence of each enantiomer at each position was determined and compared with the regions of maximum enantiodiscrimination. It can be concluded that the enantiomers tend to remain inside the CyD cavity for the longest period in the simulation, forming stable complexes. However the preferential binding sites for *R*- and *S*-equol are different and do not correspond to the regions of maximum chiral discrimination, therefore we can conclude that β-CyD is not the optimal chiral stationary phase for equol, despite the magnitude of the energy difference.

Acknowledgments We are grateful to the Ministerio de Educación y Ciencia and FEDER (FIS2005-02886) for their generous financial support.

References

1. Allen, M.P., Tildesley, D.J.: Computer Simulation of Liquids. Clarendon Press, Oxford (1987).
2. Allen, M.P., Tildesley, D.J.: Computer Simulation in Chemical Physics. Kluwer Academic Publishers, Dordrecht (1993).
3. Leach, A.R.: Molecular Modelling. Principles and Applications. Addison Wesley Longman Limited, Essex (1996).
4. Rapaport, D.C.: The art of Molecular Dynamics Simulation. Cambridge University Press, Cambridge (1995).
5. Szejtli, J.: Cyclodextrins and their Inclusion Complexes. Akademiai Kiado, Budapest (1982).
6. Menges, R.A., Armstrong, D.W.: Chiral Separations by Liquid Chromatography. Am. Chem. Soc. Washington (1991).
7. Lipkowitz, K.B.: Theoretical studies of type II–V chiral stationary phases. J. Chromatogr. A **694**, 15–37 (1995).
8. Lipkowitz, K.B.: Applications of computational chemistry to the study of cyclodextrins. Chem. Rev. **98**, 1829–1874 (1998).
9. Alvira, E., Mayoral, J.A., García, J.I.: A model for the interaction between β-cyclodextrin and some acrylic esters. Chem. Phys. Lett. **245**, 335–342 (1995).
10. Alvira, E., Cativiela, C., García, J.I., Mayoral, J.A.: Diels-Alder reactions in β-cyclodextrin cavities. A molecular modelling study. Tetrahedron Lett. **36**, 2129–2132 (1995).
11. Alvira, E., Mayoral, J.A., García, J.I.: Molecular modelling study of β-cyclodextrin inclusion complexes. Chem. Phys. Lett. **271**, 178–184 (1997).
12. Alvira, E., García, J.I., Mayoral, J.A.: Molecular modelling study for chiral separation of equol enantiomers by β-cyclodextrin. Chem. Phys. **240**, 101–108 (1999).
13. Alvira, E., García, J.I., Mayoral, J.A.: Factors influencing β-cyclodextrin inclusion complex formation. Recent Res. Dev. Chem. Physics **1**, 89–100 (2000).
14. Alda, J.O., Mayoral, J.A., Lou, M., Jiménez, Y., Martinez, R.M., Garay, R.P.: Purification and chemical characterization of a potent inhibitor of the Na-K-Cl cotransport system in rat urine. Biochem. Biophys. Res. Commun. **221**, 279–285 (1996).
15. Lipkowitz, K.B., Pearl, G., Coner, B., Peterson, M.A.: Explanation of where and how enantioselective binding takes place on permethylated β-cyclodextrin, a chiral stationary phase used in gas chromatography. J. Am. Chem. Soc. **119**, 600–610 (1997).
16. Lipkowitz, K.B., Coner, B., Peterson, M.A.: Locating regions of maximum chiral discrimination: a computational study of enantioselection on a popular chiral stationary phase used in chromatography. J. Am. Chem. Soc. **119**, 11269–11276 (1997).
17. Allinger, N.L.: Conformational analysis. 130. MM2. A hydrocarbon force field utilizing V1 and V2 torsional terms. J. Am. Chem. Soc. **99**, 8127–8134 (1977).
18. Burkert, U., Allinger, N.L.: Molecular mechanics, ACS Monographs 177. Am. Chem. Soc., Washington (1982).
19. Weiner, S.J., Kollman, P.A., Case, D.A., Singh, U.C., Ghio, C., Alagona, G., Profeta, S., Weiner, P.J.: A new force field for molecular and mechanical simulation of nucelic acids and proteins. J. Am. Chem. Soc. **106**, 765–784 (1984).
20. Weiner, S.J., Kollman, P.A., Nguyen, D.T., Case, D.A.: J. Am. Chem. Soc. **108**, 230 (1986).
21. Macromodel V5.0, Department of chemistry, Columbia University (1995).
22. Hasel, W., Hendrickson, T.F., Still, W.C.: A rapid approximation to the solvent accessible surface areas of atoms. Tetrahedron Comput. Methodol. **1**, 103–116 (1988).
23. Still, W.C., Tempczyk, A., Hawley, R.C., Hendrickson, T.F.: Semianalytical treatment of solvation for molecular mechanics and dynamics. J. Am. Chem. Soc. **112**, 6127–6129 (1990).
24. Klingert, B., Rihs, G.: Molecular encapsulation of transition metal complexes in cyclodextrins. Part 3. Structural consequences of varying the guest geometry in channel-type inclusion compounds. J. Chem. Soc. Dalton Trans. 2749–2760 (1991).
25. Stewart, J.J.P.: MOPAC 6.0, QCPE 455 (1990).
26. Brown, D., Clarke, J.H.R.: A comparison of constant energy, constant temperature and constant pressure ensembles in molecular dynamics simulations of atomic liquids. Mol. Phys. **51**, 1243–1252 (1984).
27. Fincham, D., Quirke, N., Tildesley, D.J.: Computer simulation of molecular liquid mixtures. I. A diatomic Lennard-Jones model mixture for CO_2/C_2H_6. J. Chem. Phys. **84**, 4535–4546 (1986).